

A Novel Approach to the Design of an Artificial Bionic Baroreflex

Pedram Ataee, Guy A. Dumont, Hossein A. Noubari, W. Thomas Boyce, J. Mark Ansermino

Abstract—This paper presents a computationally efficient method to design an artificial bionic baroreflex. This work is built upon a physiology-based mathematical model of autonomic-cardiac regulation describing the regulation of heart rate and blood pressure as well as a system identification technique to identify a subject-specific mathematical model for each subject. The control strategy to regulate blood pressure is developed based upon the in-vivo baroreflex mechanism. A unique strength of the proposed method is its capability to determine the modulating baroreflex functions on the sympathetic and parasympathetic nerve activities. This method can be used in the treatment of individuals with baroreflex failure through overriding the corresponding nerves to properly regulate blood pressure. In fact, nerve overriding causes heart rate and arterial stiffness to adjust such that blood pressure reaches a proper range to provide enough oxygenated-blood to the critical organs.

I. INTRODUCTION

The autonomic-nervous system (ANS) maintains homeostasis in the cardiovascular system (CVS) through many negative feedback mechanisms including the baroreflex (the major short-term blood pressure control mechanism) to deliver adequate oxygenated blood-flow to organs against physical (e.g. exercise and orthostatic hypotension) and psychological (e.g. fear and anxiety) stressors [1]–[3].

In the CVS, the instantaneous arterial blood pressure (BP) is sensed by baroreceptors located on the major arteries. Accordingly, a series of commands are produced by the baroreflex and transmitted to the heart, arteries, and other organs to maintain homeostasis in the CVS. An artificial bionic baroreflex consists of pressure sensors to measure arterial BP, and a neurostimulator generating an electrical pulse train to stimulate sympathetic and parasympathetic nerves regulated by a computerized device [4], [5].

The gravitational effect on circulation during postural changes provokes a baroreflex response to prevent hypotension and hypoperfusion of the brain [6]. Therefore, baroreflex failure in individuals with severe orthostatic hypotension (e.g., individuals with traumatic spinal cord injuries) may result in loss of consciousness during sitting to standing position change resulting in severely impaired quality of life [5], [7]. Moreover, the prevalence of drug-resistant hypertension (i.e., BP remains above 140/90 mmHg in spite of the concurrent

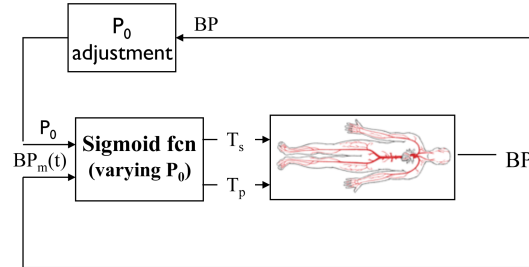


Fig. 1. Schematic model of autonomic-cardiac regulation with emphasis on the baroreflex

use of 3 anti-hypertensive medications [8], [9]) has increased in the recent years [8], [10]. An artificial bionic baroreflex is aimed to be an effective treatment for baroreflex failure in individuals with drug-resistant hypertension and severe orthostatic hypotension.

In [6], the open-loop transfer function of the baroreflex was identified using white noise pressure perturbation after anatomically isolating the carotid sinuses by assuming that the baroreflex works linearly in some physiological pressure range. Kawada and Sugimachi [7] present encouraging results to prevent orthostatic hypotension in anesthetized cats using epidural spinal cord stimulation and frequency analysis. The nerve stimulation devices can be implanted or percutaneously inserted into the skin surface.

We propose a method to design an artificial bionic baroreflex by mimicking the in-vivo baroreflex mechanism, which can be used in adjusting the existing neurostimulator devices to regulate BP within an individual's CVS (Fig. 1). The proposed method consists of two parts: a sigmoidal characteristic to mimic the modulating baroreflex functions on the sympathetic and parasympathetic nerve activities, and an adaptation mechanism adjusting the sigmoidal characteristic to different physiological conditions (e.g., exercise and sleep), as well as pathological conditions (e.g., hypertension and cardiovascular disorders). The adaptation mechanism resetting the baroreflex characteristic is devised according to the physiological adjustment mechanism of the in-vivo baroreflex.

II. METHODS AND ALGORITHM

In this section, we first briefly explain the experimental data obtained from the MIMIC dataset which is used in this study. We then present a physiology-based mathematical model of the autonomic-cardiac regulation described by two coupled non-linear, delay-differential equations. Subsequently, the system identification technique introduced in [11] and used to develop subject-specific models for 3 subjects is briefly explained. In this study, the subject-specific mathematical model has

P. Ataee and G.A. Dumont are with the Department of Electrical and Computer Engineering, The University of British Columbia, Vancouver, Canada (pedrama@ece.ubc.ca).

H.A. Noubari is with the Department of Electrical and Computer Engineering, The University of British Columbia, Vancouver, Canada, and also with the School of Electrical and Computer Engineering, The University of Tehran, Tehran, Iran.

J. Mark Ansermino is with the Department of Anesthesiology, Pharmacology and Therapeutics, The University of British Columbia, Vancouver, Canada.

W.T. Boyce is with the Faculty of Medicine, The University of British Columbia, Vancouver, Canada.

TABLE I
MODEL PARAMETERS OF AUTONOMIC-CARDIAC REGULATION.

Parameter	Definition	Nominal Value
C_a	arterial compliance	1.55 mlmmHg^{-1}
R_a^0	minimum arterial resistance	0.6 mmHgsm^{-1}
ΔV	stroke volume	50 ml
H_0	intrinsic heart rate	100 min^{-1}
τ	sympathetic delay	3 s
V_H	vagal tone	1.17 s^{-2}
β_H	sympathetic control of HR	0.84 s^{-2}
α	sympathetic effect on R_a	1.3
δ_H	relaxation time	1.7 s^{-1}

been used instead of an individual's in-vivo autonomic-cardiac regulation (Fig 2). Finally, the proposed method to design an artificial bionic baroreflex is described.

A. Experimental Data

We examined the proposed method using the experimental data of autonomic-cardiac regulation in 3 subjects taken from the MIMIC Dataset [12]. A 1-hour sample of heart rate (HR) and BP signals in each individual is extracted and divided into 30s-long data segments to be used in the system identification section. The MIMIC dataset contains physiologic signals including HR, BP, and cardiac output (CO) in different lengths continuously recorded at approximately 1Hz from intensive care unit (ICU) monitors. The MIMIC dataset is freely available on the PhysioNet website [13].

B. Mathematical Model

We introduced a physiology-based mathematical model of the autonomic-cardiac regulation in [11] using two coupled differential equations (1)-(2) having nonlinear and delayed dynamic interactions, each of which describes the dynamics of HR and BP regulation as follows:

$$\dot{H}(t) = \beta_H T_s - V_H T_p + \delta_H [H_0 - H(t)] \quad (1)$$

$$\dot{P}(t) = -\frac{P(t)}{R_a^0(1 + \alpha T_s)C_a} + \frac{H(t)\Delta V}{C_a} \quad (2)$$

where H is HR, and P is mean arterial BP. The definitions and nominal values of the parameters in (1)-(2) are summarized in Table I. In this model, the modulating baroreflex functions on the sympathetic and parasympathetic nerve activities are denoted by T_s and T_p , respectively.

The modulating baroreflex functions on the sympathetic and parasympathetic nerve activities (i.e., T_s and T_p) can be modeled using a sigmoid function $\sigma(P)$ with an amplitude-limiting characteristic [14]. $\sigma(P)$ is defined as follows:

$$\sigma(P) = \frac{1}{1 + e^{-\alpha_{sp}(P - P_{sp})}} \quad 50 \leq P \leq 200. \quad (3)$$

The sigmoid function $\sigma(P)$ is characterized using two variables, setpoint P_{sp} and sensitivity α_{sp} [15], [16]. To simulate the in-vivo sympathetic and parasympathetic modulating functions, we substitute $T_s = 1 - \sigma(P(t - \tau))$ and $T_p = \sigma(P(t))$ into (1)-(2).

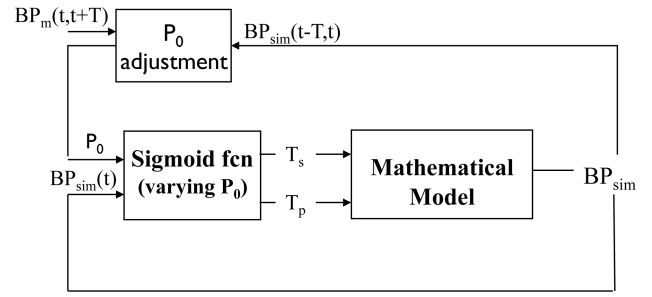


Fig. 2. Schematic model of the proposed artificial bionic baroreflex

Parametric sensitivity analysis is conducted on the model to classify the model parameters into high-sensitivity and low-sensitivity groups based on their relative impacts on the system outputs. H_0 and R_a^0 were initially classified into the category of “invariant” parameters since they are essentially constant within an individual in a short-time interval. The remaining model parameters were classified into high-sensitivity (V_H , β_H , α , ΔV , and P_0) and low-sensitivity (α_{sig} , γ , C_a , τ , δ_H) groups according to the results of the sensitivity analysis to select a subset of parameters with significant impact on the system outputs (i.e., high-sensitivity group). The detailed description of the mathematical model and parametric sensitivity analysis is explained in [11].

C. System Identification

To estimate subject-specific high-sensitivity parameters in (1)-(2), a system identification method was developed based on an optimization problem minimizing the normalized L_1 -error between measured versus model-estimated HR and BP signals. The system identification was performed by optimizing the high-sensitivity parameters such that the error function (4) become minimized in each 30s-long data segment, whereas low-sensitivity and invariant parameters were fixed at their corresponding population nominal values (Table I). The error function (i.e., the objective function) was specified as follows:

$$J = \frac{E_P + E_H}{2}; \quad E_X = \sum_{t=0}^n \left| \frac{X_s(t, \Gamma) - X_m(t)}{X_m(t)} \right|, \quad (4)$$

where $X_m(t)$ and $X_s(t, \Gamma)$ ($X = H, P$) are measured and model-estimated output signals, respectively, and $\Gamma = \{V_H, \beta_H, \alpha, \Delta V, P_0, \alpha_{sig}, \gamma, C_a, \tau, \delta_H, H_0, R_a^0\}$. The optimization problem was solved using the fmincon routine with an active-set algorithm in the MATLAB Optimization Toolbox [17] which finds the constrained minimum of a multivariable nonlinear scalar function J using Quasi-Newton approximation. The set of optimized high-sensitivity parameters minimizing the error function were used as representative (or, estimates) of high-sensitivity parameters for the corresponding data segment. The system identification method has been thoroughly described in [18].

D. Artificial Bionic Baroreflex

The measured BP (BP_m) must be continuously compared to the time-varying BP setpoints (BP_{sp}), i.e., the BP level providing the need of body organs for oxygenated-blood. If the BP_m differs from the BP_{sp} , the baroreflex characteristic is adjusted such that it causes the BP to gradually reach the BP_{sp} . In this study, individuals were replaced by subject-specific mathematical models describing autonomic-cardiac regulation of each subject, simulated BP (BP_{sim}) instead of BP_m is continuously compared against the BP_{sp} . The baroreflex effects on the autonomic-cardiac regulation are achieved by modulating sympathetic and parasympathetic nerve activities (V_H , β_H , and α) using T_s and T_p . Therefore, for example, when the BP must decrease to reach the setpoint, T_p must reset such that its magnitude at the same BP level becomes higher. This causes HR decreases and then BP decreases. Considering T_p is a sigmoidal curve, P_0 must reset to a lower value in order to obtain a higher HR decelerating parasympathetic effect and vice versa. Therefore, P_0 , then sigmoidal characteristic, must be updated by the adjustment rule as follows:

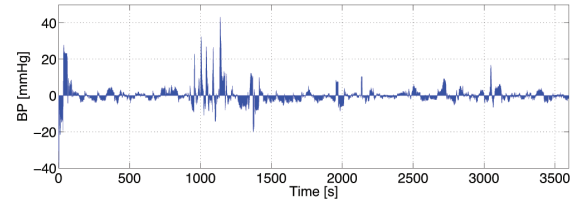
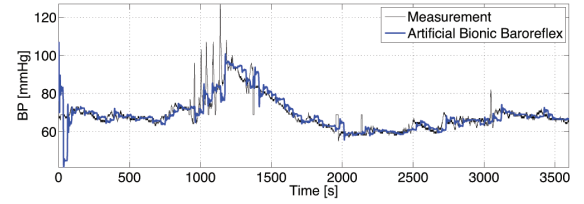
$$P_0(t + \Delta) = P_0(t) + k \cdot (BP_m - BP_{sp}) \quad (5)$$

where k is a positive coefficient representing pace or strength of the adjusting mechanism to an error in the BP regulation, and Δ is an interval in which the baroreflex characteristic needs to be updated. The adjustment rule (5) is initialized by $P_0 = 100$. Moreover, to be consistent with the baroreflex physiology, the P_0 is constrained between 50 mmHg and 200 mmHg. A very large k may cause overshoot in the control system while a very small k may cause a large settling time preventing proper adjustment of baroreflex characteristic to track the BP_{sp} . This coefficient is empirically tuned to $k = 0.08$ by considering both overshoot and settling time of the control system. The time interval Δ in (5) is 30s in this study; however, it can be set to a larger or smaller value depending on the pace of variation in BP_{sp} .

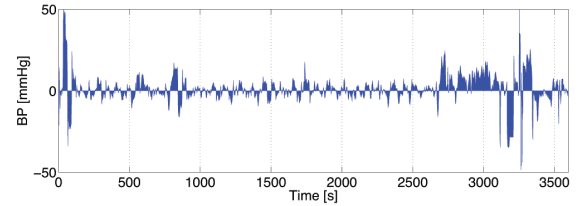
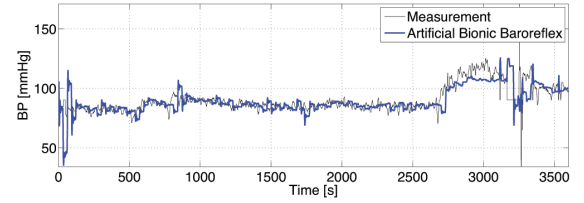
III. RESULTS AND DISCUSSION

Since we aimed to use a subject-specific mathematical model for each individual, the mathematical model (1)-(2) was specified by estimating individualized nominal values for high-sensitivity parameters in each subject whereas the remaining parameters were assigned by their population nominal values (Table I). As the MIMIC dataset contains CO measurement, we therefore calculated an individualized nominal value of ΔV for each subject instead of either estimating ΔV by the proposed identification technique or using the population nominal value. Accordingly, we obtained time series of V_H , β_H , and α with a 1-hour length using the system identification technique, and the average value of these parameters over 1-hour length were calculated to be assigned as individualized nominal values (Table II). Note that the individualized high-sensitivity parameters must be updated every 1-hour (or, any other length initially assumed) interval of data in the future studies. We obtained 3 sets of model parameters representing 3

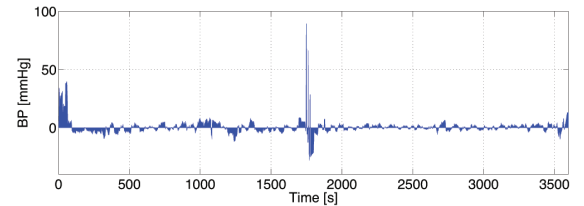
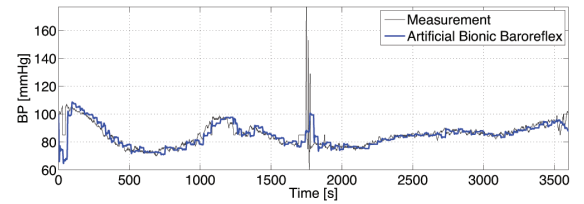
subjects in the 1-hour interval to evaluate the proposed method in designing an artificial bionic baroreflex.



(a) Case No.: 477



(b) Case No.: 486



(c) Case No.: 476

Fig. 3. BP measurement (BP setpoint) vs. the results of the artificial bionic baroreflex (simulated BP) for 3 subjects with subject ID: 477, 486, and 476.

TABLE II
INDIVIDUALIZED NOMINAL VALUES OF HIGH-SENSITIVITY PARAMETERS
IN 3 SUBJECTS VERSUS CORRESPONDING POPULATION NOMINAL VALUES

	Subject			Population
	I (477)	II (486)	III (476)	
V_H	0.65	1.37	2.13	1.17
β_H	1.5	0.87	0.68	0.84
α	0.7	1.36	1.55	1.3
ΔV	46	40	36	50

To evaluate the proposed method, we compared the simulated BP obtained based on the control strategy (5) versus the BP setpoints (Fig. 3). In each panel of Fig. 3, the top figure shows the BP measurement used as BP setpoints versus simulated BP obtained by the proposed artificial bionic baroreflex and the bottom figure shows the tracking error over the 1-hour interval. In each subject shown in Fig. 3, the tracking error is considerably higher during $t = 0s - 100s$ due to the P_0 initialization. After $t > 100s$, P_0 converges to a proper value to control the BP regulation system. Since we assumed that the control strategy would not respond very rapidly, several abrupt changes in the BP setpoints during $t = 1000s - 1300s$ in Fig 3(a) and $t = 1700s - 1800s$ in Fig 3(c) which may be originated due to the measurement noise caused the tracking error to become large. Fig 4 shows the calculated P_0 for 3 subjects. Considering the large tracking error between $t = 2700s$ and $t = 3200$ in Fig 3(b) and the saturated P_0 at 200 during the same interval, it can be concluded that the control strategy was not able to track the setpoints successfully in that interval.

IV. CONCLUSIONS AND FUTURE WORK

In conclusion, this paper presented the feasibility and potential for a computationally efficient method to design an artificial bionic baroreflex that can be used in the treatment of baroreflex failure. Future work will include the evaluation and validation of the real-time performance of the proposed approach in clinical settings, e.g., the system identification strategy may need to be adjusted due to the activation of the bionic baroreflex in the clinical setting.

REFERENCES

- [1] A. Dudkowska and D. Makowiec. Seidel-Herzel model of human baroreflex in cardiorespiratory system with stochastic delays. *Journal of Mathematical Biology*, 57:111–137, 2008.
- [2] R.A.L. Dampney, J. Horiuchi, and L.M. McDowall. Hypothalamic mechanisms coordinating cardiorespiratory function during exercise and defensive behaviour. *Autonomic Neuroscience: Basic & Clinical*, 142(1-2):3–10, 2008.
- [3] J.L. Elghozi and C. Julien. Sympathetic control of short-term heart rate variability and its pharmacological modulation. *Fundamental & Clinical Pharmacology*, 21(4):337–47, 2007.
- [4] K. Hosokawa, T. Ide, T. Tobushi, K. Sakamoto, K. Onitsuka, T. Sakamoto, T. Fujino, K. Saku, and K. Sunagawa. Bionic baroreceptor corrects postural hypotension in rats with impaired baroreceptor. *Circulation*, 126(10):1278–85, 2012.
- [5] T. Sato, T. Kawada, T. Shishido, M. Sugimachi, J. Alexander, and K. Sunagawa. Novel Therapeutic Strategy Against Central Baroreflex Failure : A Bionic Baroreflex System. *Circulation*, 100(3):299–304, 1999.

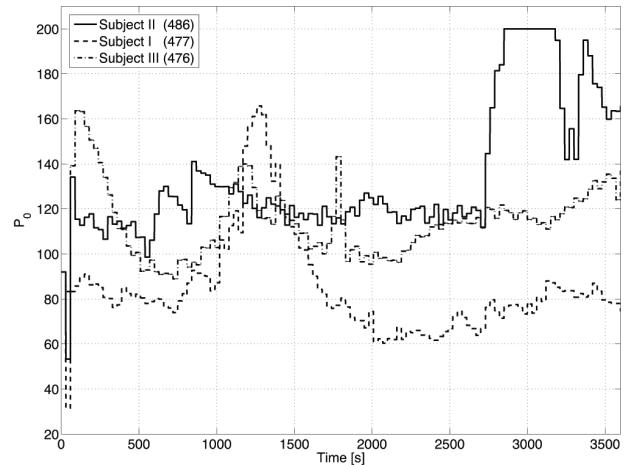


Fig. 4. The calculated control signal P_0 in 3 subjects

- [6] K. Sunagawa and M. Sugimachi. Development of artificial bionic baroreflex system. In *Proceedings of the 32nd Annual International Conference of the IEEE EMBS*, volume 2010, pages 3446–8, 2010.
- [7] T. Kawada and M. Sugimachi. Artificial neural interfaces for bionic cardiovascular treatments. *Journal of Artificial Organs*, 12(1):17–22, 2009.
- [8] D.A. Calhoun, D. Jones, S. Textor, D.C. Goff, T.P. Murphy, R.D. Toto, A. White, W.C. Cushman, W. White, D. Sica, K. Ferdinand, T.D. Giles, B. Falkner, and R.M. Carey. Resistant hypertension: diagnosis, evaluation, and treatment. A scientific statement from the American Heart Association Professional Education Committee of the Council for High Blood Pressure Research. *Hypertension*, 51(6):1403–19, 2008.
- [9] J.D. Filippone and J.D. Bisognano. Baroreflex stimulation in the treatment of hypertension. *Current Opinion in Nephrology and Hypertension*, 16(5):403–8, 2007.
- [10] S.D. Navaneethan, T.E. Lohmeier, and J.D. Bisognano. Baroreflex stimulation: A novel treatment option for resistant hypertension. *Journal of the American Society of Hypertension : JASH*, 3(1):69–74, 2009.
- [11] P. Ataei, J.O. Hahn, C. Brouse, G.A. Dumont, and W.T. Boyce. Identification of cardiovascular baroreflex for probing homeostatic stability. *Proceedings of the Computing in Cardiology*, pages 141–144, 2010.
- [12] G.B. Moody and R.G. Mark. A database to support development and evaluation of intelligent intensive care monitoring. In *Proceedings of the Computers in Cardiology*, pages 657–660, 1996.
- [13] A.L. Goldberger, L.A.N. Amaral, L. Glass, J.M. Hausdorff, P.Ch. Ivanov, R.G. Mark, J.E. Mietus, G.B. Moody, C.K. Peng, and H.E. Stanley. Physiobank, physiotookit, and physionet : Components of a new research resource for complex physiologic signals. *Circulation*, 101(23):e215–e220, 2000.
- [14] J.V. Ringwood and S.C. Malpas. Slow oscillations in blood pressure via a nonlinear feedback model. *American Journal of Physiology - Regulatory, Integrative and Comparative Physiology*, 280:R1105–15, 2001.
- [15] L.M. McDowall and R.A.L. Dampney. Calculation of threshold and saturation points of sigmoidal baroreflex function curves. *American Journal of Physiology- Heart and Circulatory Physiology*, 291(4):H2003–7, 2006.
- [16] V.L. Cooper, S.B. Pearson, C.M. Bowker, M.W. Elliott, and R. Hainsworth. Interaction of chemoreceptor and baroreceptor reflexes by hypoxia and hypercapnia - a mechanism for promoting hypertension in obstructive sleep apnoea. *The Journal of physiology*, 568(2):677–87, 2005.
- [17] *MATLAB Optimization Toolbox User's Guide*, MathWorks, 2010.
- [18] P. Ataei, J.O. Hahn, G.A. Dumont, and W.T. Boyce. Non-Invasive Subject-Specific Monitoring of Autonomic-Cardiac Regulation. *Manuscript submitted for publication*, 2013.